Science of Amorphous and Aperiodic Materials

Current Principal Investigators:
S.B. Biner (0.3 FTE)
M.J. Kramer (0.5 FTE)
T.A. Lograsso (0.1 FTE)
D.J. Sordelet (0.2 FTE)

For FY2003-2005 -

Assistant Scientists:
M.F. Besser
K.W. Dennis
A. Kracher
D. Wu

Postdoctoral Fellows: 4

Graduate Students: 1

Collaborators:
Ashraf Bastawros, Scott Chumbley, Steven Martin, and Xiaoli Tan (Iowa State University)
James Morris (Oak Ridge National Laboratory)
Walter Steurer (Swiss Federal Institute of Technology Zurich, Switzerland)
Dean Miller (Argonne National Laboratory)
Ulf Dahlborg (CNRS Laboratoire de Science et Génie des Matériaux et de Métallurgie at the Ecole des Mines de Nancy, France)
Do Hyang Kim (Yonsei University, Center for Non-Crystalline Materials, Seoul, Korea)
Jürgen Eckert (Technische Universität Darmstadt, Darmstadt, Germany)
Helena Van Swygenhoven (Paul Scherrer Institute, Villegen, Switzerland)
Ian Fisher (Stanford University)

OUTPUT SUMMARY – FY2003-2005

Invited Conference Presentations	17
Other Invited Presentations	11
Contributed Presentations	12
Journal Papers	46
Conference Papers	7

ABSTRACT AND BACKGROUND

The main scientific goals of the *Science of Amorphous and Aperiodic Materials* focus area are directed toward gaining an increased fundamental understanding of (i) the correlation between short-range atomic order and phase selection during devitrification and deformation behavior in amorphous systems and (ii) the role of crystal chemistry (i.e., composition, bonding and coordination) in controlling the structural stability of aperiodic systems. Amorphous and aperiodic structures, while nearly opposite in terms of long-range atomic order can exhibit remarkable interrelationships, particularly in regard to short-range atomic order. For instance, metastable aperiodic phases (i.e., quasicrystals) have been observed during the devitrification sequence of numerous amorphous metallic systems. Moreover, metastable phases can also form directly from the liquid during quenching of glass-forming systems. Formation of non-equilibrium phases is often speculated to occur because they have local structural units that are similar to the short- and medium-range atomic arrangements in liquids and amorphous phases. Local atomic order also influences mechanical behavior of amorphous systems where deformation occurs via the formation and propagation of shear bands. Within the shear bands, localized ductility can be very large and structural changes during deformation have been suggested, but without universal agreement, to include strain-induced crystallization, local melting and evolution of free volume.

Experimental synthesis techniques are being closely coupled with dynamic structural characterization methods (e.g., time-resolved high-energy synchrotron scattering) to examine the nature, specific atomic configurations and energetics associated with the devitrification and crystallization of selected amorphous systems. Devitrification pathways leading to metastable and equilibrium phases are being examined to further understand system-specific tendencies towards metastable or stable phase selection during formation and annealing of amorphous phases. Closely linked to experimental efforts are emerging theoretical and computational studies to understand the structure and dynamics of the liquid preceding glass formation. These

efforts leverage considerably from the current theoretical and experimental research within the "*Correlations and Dynamics in Metallic Liquids*" project. Additionally, molecular dynamics and numerical simulations to describe deformation within an amorphous system are being developed and utilized to predict the source of shear band formation, together with the associated thermal and structural changes that occur during their growth.

To fully understand the intricate dynamic boundaries surrounding glass formation, non-equilibrium phase selection during devitrification or crystallization of amorphous structures and the formation of stable aperiodic and related approximant structures, it is critical to have high-purity materials together with precise synthesis techniques and high-resolution structural characterization facilities capable of data collection at high temperatures under real-time conditions. Moreover, it is very desirable to develop predictive capabilities using computation, simulation and theoretical approaches that can be compared with experimental results. Ames Laboratory has a unique array of high-purity material preparation and synthesis techniques that are being coupled with advanced characterization techniques and theoretical approaches available through existing, active collaborations, particularly involving DOE-BES-supported user facilities.

During the last three years this research focus area has involved the following four highly focused, yet thoroughly integrated scientific efforts. "*Local Atomic Clusters in Metallic Glasses* M. J. Kramer," is designed to utilize recent advances in time-resolved high-temperature X-ray diffraction techniques in conjunction with pair distribution analysis and Reverse Monte Carlo simulations to more fully understand as-synthesized and evolving structures. Variations in local atomic order are examined from glass formation through devitrification with the ultimate goal of identifying specific links between the structure of the liquid and the amorphous state. As many amorphous metallic alloys are obtained by rapid quenching from the liquid, this work also includes an effort to probe the structure of the starting liquid. "*Linkages between Atomic Structure of Liquids and Metastable Phase Formation in Amorphous Metallic Systems* D. J. Sordelet," seeks to elucidate the formation, stability and transformation behaviors of metastable devitrification and crystallization phases. Special emphasis is directed towards establishing a linkage between the short- and medium-range atomic structure of the amorphous state and the ensuing devitrification phases. In addition, alternate synthesis routes are being used to obtain amorphous phases having the same composition, but different atomic structures to further separate chemical and topological order effects on crystallization pathways. "*Modeling and Simulation of Homogeneous and Inhomogeneous Deformation Behavior of Metallic Glasses* S. B. Biner," is a groundbreaking study employing numerical and molecular dynamics simulations to understand the structural dependencies and underlying mechanisms that are responsible for controlling the different possible deformation modes in metallic glasses and their composites. This work is closely supported by experimental mechanical testing efforts to help validate and refine simulations as well as by advanced characterization methods to test predictions of deformation-induced structural evolution. The work in "*Synthesis and Phase Relations of Binary Quasicrystalline and Approximant Phases* T. A. Lograsso," is examining the phase stability differences between aperiodic and crystalline materials. Here, the unique, world-class single-crystal growth capabilities at Ames Laboratory are extensively utilized. In particular, successful recent efforts to synthesize "perfect" single grains of binary Cd-based quasicrystalline and related approximant phases have allowed several unprecedented experiments to be performed.

The Research Highlights in the following pages provide several examples from these four primary projects that are collectively aimed at contributing to the scientific goals of this research focus area.

TECHNICAL HIGHLIGHTS

- Direct validation of *ab initio* calculations of a metastable state in a narrow Zr-(Pd,Cu)

composition range using high-energy X-ray diffraction.

- Correlation of the local atomic structure in the $Cd_{84}Yb_{16}$ quasicrystal and its $Cd_{86}Yb_{14}$ cubic approximant using high-resolution transmission electron microscopy.
- Demonstrated that quasicrystalline $Cd_{84}Yb_{16}$ melts and solidifies congruently and determined its liquid structure using *in-situ* X-ray diffraction.
- Using time-resolved high-energy X-ray diffraction, discovered that phase selection in Zr-Pt alloys during solidification from the liquid and devitrification from an amorphous phase changes from stable to metastable with < 1 at% change in composition.
- Direct observation of the amorphous structure of a shear band formed under room temperature compressive loading in a Zr-based bulk metallic glass.
- Demonstrated that metastable quasicrystal phase formation during annealing of metallic glasses is also possible in amorphous structures synthesized by solid-state and physical vapor deposition routes, revealing that a specific liquid structure preceding vitrification is not required.
- Developed a novel refractory metal/metallic glass composite powder synthesis technique to fabricate monolithic structures having nano-scale layers of each phase resulting in global shear localization not previously obtained with materials involving bcc-metals.
- Performed molecular dynamics and finite element simulations to determine that a pressure-dependent yield surface is dominant during deformation of metallic glasses.
- Numerical analyses of failure behavior in metallic glass composites with ductile reinforcements agree with experimental results and indicate that ductility is intrinsically controlled only by the matrix with very little influence from the reinforcement.
- Two-dimensional molecular dynamics simulations of a model metallic glass shows that the presence of two creep regimes, Newtonian flow and power-law creep, is associated with the evolution of free volume and the predictions were confirmed by experiments.
- Utilized high-energy two-dimensional synchrotron scattering studies to reveal anisotropic free volume formation during homogeneous deformation of highly-strained (>70%) metallic glasses.
- Molecular dynamics simulations of nano-indentation of a model metallic glass indicate that a temperature rise does occur under the indenter, but remains below the glass transition temperature indicating that any crystalline phase formation seen in experiments is not necessarily associated with temperature evolution during the course of deformation.
- Developed synthesis methods to obtain high-quality single crystals of quasicrystals and approximants in Cd-Yb and other binary alloys systems.
- Prepared well-oriented single crystals with precise compositions to facilitate measuring elastic constants and thermal expansion for $Cd_{84}Yb_{16}$ and $Cd_{51}Yb_{14}$ alloys, which led to the first-ever observation of a low-temperature, first-order phase transition in hexagonal $Cd_{51}Yb_{14}$.
- Synthesized natural and isotopic Cd-Yb with precise compositions along with a sophisticated containment system for neutron and x-ray scattering studies.

INTERACTIONS WITH OTHER PROJECTS AND PROGRAMS

This work will continue to be part of a broader effort in both the Materials and Engineering Physics and Materials Chemistry Programs to understand the linkages between short-range order (e.g., possible icosahedral coordination) in the liquid and amorphous states and the formation of quasiperiodic structures. There will be ongoing efforts to develop and refine

structural models based on reverse Monte Carlo simulations; moreover, additional constraints such as accurate interatomic potentials under development in the *Correlation and Dynamics in Metallic Liquids* subtask will be introduced into our Monte Carlo simulations. In addition, our collaboration with J. Morris at Oak Ridge National Laboratory will be expanded to include the Cd-Yb system, where he is starting with simple Lennard-Jones potentials to perform molecular dynamics simulations that attempt to approximate our scattering experiments.

SELECTED PUBLICATIONS

M.J. Kramer and D.J. Sordelet, "Polymorphism in the Short-Range Order of $Zr_{70}Pd_{30}$ Metallic Glasses," J. Non-Cryst. Solids, **351,** 1586 (2005).

M.H. Lee, X.Y. Yang, M.J. Kramer, and D.J. Sordelet, "Glass Formation and Crystallization in Binary Zr-Pt Systems," Philosophical Magazine (in press).

S. Scudino, C. Mickel, L. Schultz, J. Eckert, X.Y. Yang, and D.J. Sordelet, "Quasicrystal Formation in Mechanically Alloyed Zr-Ti-Nb-Cu-Ni-Al Glassy Powders," Appl. Phys. Lett., **85**, 4349 (2004).

S. Venkataraman, S. Scudino, J. Eckert, T. Gemming, C. Mickel, L. Schultz, and D.J. Sordelet, "Nanocrystallization of $Cu_{47}Ti_{33}Zr_{11}Ni_8Si_1$ Metallic Glass," J. Mater. Res. (in press).

D.J. Sordelet, E. Rozhkova, M.F. Besser, and M.J. Kramer, "Metastable Quasicrystal Formation in Vitrified and Solid State Synthesized Amorphous Zr-based Alloys," J. Non-Cryst. Solids, **334 & 335**, 263 (2004).

D.J. Sordelet, X.Y. Yang, E.A. Rozhkova, M.F. Besser, and M.J. Kramer, "Influence of Oxygen Content in Phase Selection During Quenching of $Zr_{80}Pt_{20}$ Melt-Spun Ribbons," Intermetallics, **12**, 1211 (2004).

S.W. Martin, J. Walleser, A. Karthikeyan, and D.J. Sordelet, "Enthalpy Relaxation Studies of The Glass Transition in a Metallic Glass," J. Non-Cryst. Solids, **349**, 347 (2004).

D.J. Sordelet, E. Rozhkova, M.F. Besser, and M.J. Kramer, "Synthesis Route-Dependent Formation of Quasicrystals in $Zr_{70}Pd_{30}$ and $Zr_{70}Pd_{20}Cu_{10}$ Amorphous Alloys," Appl. Phys. Lett., **80**, 4735 (2002).

S.B. Biner, "Ductility of Bulk Metallic Glasses and Their Composites with Ductile Reinforcements: A Numerical Study," Acta Mater. (in press).

A. Antoniou, A.F. Bastawros, C.C.H. Lo, and S.B. Biner, "Deformation Behavior of a Zr-based Metallic Glass During Cylindrical Indentation: In-Situ Observations," Mater. Sci. Eng., A, **394**, 96 (2005).

M.J. Kramer, D.J. Sordelet, A.F. Bastarows, X. Tan, and S.B. Biner, "Absence of Crystallization During Cylindrical Indentation of a Zr-based Metallic Glass," J. Non-Cryst. Solids, **351**, 2159 (2005).

M.J. Kramer, T.A. Lograsso, and D.J. Sordelet, "Solid and Liquid Thermal Expansion and Structural Observations in the Quasicrystalline $Cd_{84}Yb_{16}$ Compound," Phil. Mag. Lett., **85**, 151 (2005).

J. Schreuer, W. Steurer, T.A. Lograsso, and D. Wu, "Elastic Properties of Icosahedral i-$Cd_{84}Yb_{16}$ and Its Hexagonal Approximant h-$Cd_{51}Yb_{14}$," Phil. Mag. Lett., **84**, 643 (2004).

S. Francoual, K. Shibata, M. de Boissieu, A.Q.R. Baron, S. Tsutsui, R. Currat, H. Takakura, A.P. Tsai, T.A. Lograsso, and A. R. Ross, "Experimental Study of the Dynamics of the Icosahedral CdYb Phase and Its 1/1 Periodic Approximant," Ferroelectrics, **305**, 235 (2004).

J.A. Barrow, M.C. Lemieux, B.A. Cook, A.R. Ross, V.V. Tsukruk, P.C. Canfield, and D.J. Sordelet, "Micro-Surface and Bulk Thermal Behavior of a Single-Grain Decagonal Al-Ni-Co Quasicrystal," J. Non-Cryst. Solids, **334 & 335**, 312 (2004).

Local Atomic Clusters in Metallic Glasses: Electronic Structure Effects in the Amorphous $Zr_2Cu_{1-x}Pd_x$ System

Personnel: M.J. Kramer (PI), D.J. Sordelet (PI), M. Xu (Student), and Y. Y. Ye (Asst. Scientist)

Scope:

Metallic glasses have received increased attention in the last few years. However, the fundamental understanding of such materials is still lacking, and alloy design is typically based on a few common strategies. In particular, an emphasis is placed on mixing different elemental components having different metallic radii. While these may be useful guides for experimentally improving an alloy, they do not contribute to predictive capabilities. Our approach is to develop a few simple model systems to investigate underlying critical phenomena in metallic glass formation.

Research Highlights:

We investigated composition effects within a model ternary metallic glass using a combined theoretical and experimental approach. *Ab initio* calculations were used to assess the relative enthalpy differences between possible competing phases, while the actual phase transformations were monitored using time-resolved synchrotron X-ray diffraction. Collectively, these results suggest that electronic effects dominate the phase selection process and may dominate the short-range order in the as-quenched state. Using a series of model alloys, $Zr_2Cu_{1-x}Pd_x$ (x = 0, 0.25, 0.5, 0.75 and 1), we demonstrated that a*b initio* simulations can be used to help predict phase formation in complex systems. Thermal analysis would suggest that this system should behave as a simple solid-solution. The alloys in this system can all be made amorphous by rapid solidification and share the same high temperature *C11$_b$* ($MoSi_2$-type) crystal phase yet follow different devitrication pathways. In Fig. 1 the amorphous Zr_2Cu devitrifies directly to the *C11$_b$* structure, while small amounts of Pd causes the system to first transform to a metastable, quasicrystalline structure (hereafter called the *i*-phase). Increasing Pd to x = 0.5 leads to the formation of a metastable *C16* (Al_2Cu-type) structure prior to the *C11$_b$* phase. Yet for higher Pd contents, the *C16* phase is no longer observed. These results suggest an interesting competition between size and charge in the thermodynamic stability of the *C11$_b$* and *C16* phases.

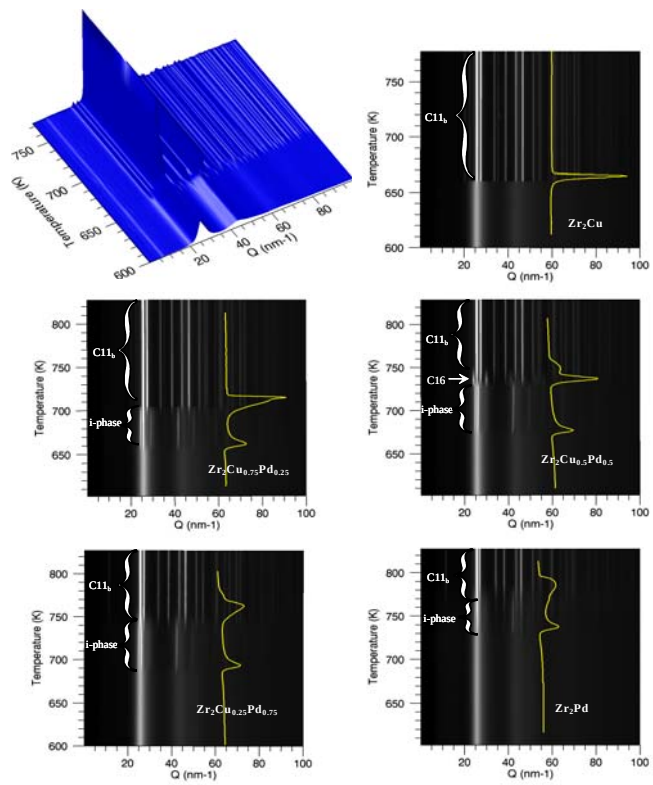

Fig. 1 Top left, a 3D representation of the time-resolved XRD patterns obtained during devitrification of the amorphous Zr_2Cu alloy. The next five images are a 2D representations of the XRD data (bright regions indicate stronger scattering intensity) of the 5 $Zr_2Cu_{1-x}Pd_x$ (x = 0, 0.25, 0.5, 0.75 and 1) alloys. The light yellow lines DSC data obtained at the same 10 K/min heating rate. All structures are amorphous at 600 K.

Electronic structure calculations were used to examine the total energies of the competing crystalline structures. The small number of components makes these alloys easier to study theoretically, and the compositions have been specifically chosen to match with supercell first-principles calculations of the competing crystal structures. In all cases the lowest energy structure was found to be the $C11_b$ phase, which is consistent with experiments.

The results of the total energies as a function of composition minus the interpolated enthalpy of the end-member compounds are shown in Fig. 2, where a convex envelope represents the stable phases. For the stable $C11_b$ structure, all calculations are close to the energy predicted for a linear interpolation of the end-members. At $x = 0.5$, we have considered two different orderings of Cu and Pd. Changing the ordering of the Cu and Pd only slightly modified the total enthalpy. The energy difference between these orderings is quite small so the Cu and Pd atoms will be disordered at ambient temperatures. This easy disordering also suggests that the size difference between Pd and Cu (about 7%) does not play a role in their stability. A stronger trend is shown for the energetics of the metastable *C16* structure. The minimum at $x = 0.5$ lowers the total energy and maximizes the entropy of mixing, indicating that the Cu and Pd will not phase separate. The results for the energies of the $NiTi_2$ structure, which contains local regions having icosahedral order, show that the energy difference is much greater than the *C16* phase. Since the energy at $x = 0.5$ is significantly higher than the average of the binaries, the system will lower its total energy by forming separate phases this structure. Therefore the $NiTi_2$ structure is *not* closely related to the *i*-phase in this system.

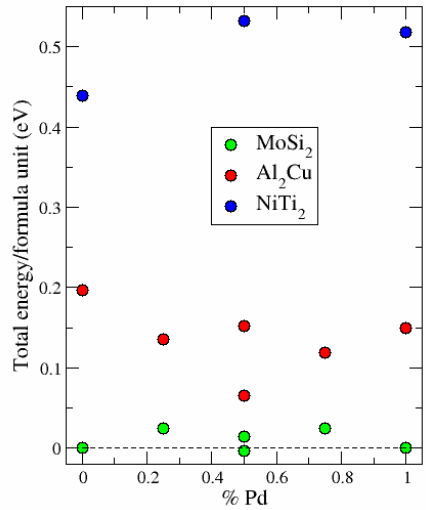

Fig. 2 Total Energy *Ab inito* calculations for possible devitrified phases in the $Zr_2Cu_{1-x}Pd_x$ (x = 0, 0.25, 0.5, 0.75 and 1) system.

Significance:

This is the first demonstration that devitrification pathways may be understood purely from theoretical considerations of the competing crystalline structures. For the alloys studied, this competition is dominated by electronic structure effects in the metastable phases. The stable crystal phase is shown to be unaffected by atomic size effects, chemical phase separation or other factors.

Future Work:

A remaining challenge in the $Zr_2Cu_{1-x}Pd_x$ system is to understand correlations between changes in the short-range order in the as-quenched alloy and the formation of the metastable quasicrystalline *i*-phase as a function of Pd content. In the absence of precise knowledge of the *i*-phase structure, it is difficult to understand the strong effect of Pd on the formation of this phase. Presumably, the nucleation of the quasicrystalline phase from the amorphous state is favored due to its lower interfacial free energy. Either the *i*-phase is strongly stabilized by small amounts of Pd or the local structure of the amorphous state is sensitive to the Pd content.

Interactions:

The *ab initio* studies of defect structures were performed with James Morris at Oak Ridge National Laboratory. The synchrotron XRD work was performed at the Advanced Photon Source.

Metastable Phase Formation in Metallic Glasses: Linkage to Atomic Structure of Liquid and Amorphous Phases

Personnel: D.J. Sordelet (PI), M.J. Kramer (PI), M.F. Besser (Asst. Scientist), X. Yang (Post Doc), and M.H. Lee (Post Doc)

Scope:

Various metallic glasses exhibit extended non-equilibrium behavior by transforming from an amorphous state into a non-equilibrium structure upon heating before ultimately transforming into a stable structure. In some systems the same metastable phase can form directly upon cooling from the liquid at a range of rates, indicating a direct linkage to liquid structure. This project examines the formation, stability and transformation of metastable phases in amorphous structures having similar compositions but formed by different synthesis routes. In particular, special emphasis is directed toward searching for a linkage between the atomic structure of the liquid and amorphous states and the ensuing devitrification phases.

Research Highlights:

Many metallic glasses form intermediate non-equilibrium phases such as the icosahedral quasicrystalline (QC) structure. These observations lead to frequent speculation that icosahedral short-range order (ISRO) exists in certain liquids, which is then retained in metallic glass state. Evidence for ISRO in undercooled liquids has been observed by Holland-Moritz[1] based on the argument of decreased interfacial energy between icosahedral solidification phases and the melt in comparison to other polytetrahedral configurations and the melt. Reports by Saida et al.[2] using TEM and DSC analyses to investigate Zr-base metallic glasses strongly infer that ISRO is present in the amorphous structure and evolves to a meta-stable QC phase. Kelton et al.[3] have coupled high-energy XRD with liquid levitation methods to further show evidence suggesting the presence of ISRO in liquid Ti-Zr-Ni alloys.

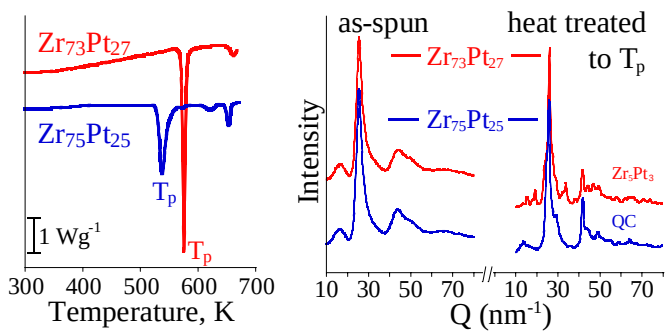

A long-range goal of this project is to gain a deeper understanding of the linkages between SRO in liquid, amorphous and metastable phases. Currently, we are examining the role of SRO in amorphous near- and off-eutectic Zr-Pt alloys (eutectic between Zr_5Pt_3 and Zr) synthesized as melt spun ribbons (MSR) and magnetron sputtered films; the latter synthesis method is used to search for structural and transformation differences in amorphous structures that did not form directly from a liquid. As illustrated above, DSC and XRD data reveal a slight change in composition leads to very different devitrification behaviors of Zr-Pt MSR. The XRD data from the as-spun ribbons are comparable, but the DSC of the $Zr_{75}Pt_{25}$ MSR shows a lower initial transformation temperature and additional exothermic peaks at higher temperatures. Heating the ribbons to the first peak temperature, T_p. illustrates the contrasting devitrification pathways. The $Zr_{75}Pt_{25}$ MSR forms a metastable QC phase, while the $Zr_{73}Pt_{23}$ MSR transforms directly to the equilibrium Zr_5Pt_3 phase. Furthermore, when these two alloys were melt spun at lower wheel speeds, they exhibited solidification behavior that was comparable to their devitrification behavior. This is very compelling evidence that subtle composition changes have a very potent effect on the structure and transformation behavior of metallic glass-forming liquids.

While the formation of a metastable QC phase during crystallization of amorphous Zr-Pt requires an appropriate composition, we found that it is not necessary that the amorphous phase be obtained directly from a liquid. High-energy, time-resolved X-ray diffraction data obtained at the Advanced Photon Source clearly illustrates the transform behavior of $Zr_{80-x}Pt_x$ magnetron sputtered films (MSF). The above 2-dimensional presentation of the diffraction data and selected XRD scans at specific temperatures illustrate the contrasting crystallization behavior of amorphous $Zr_{73}Pt_{27}$ and $Zr_{77}Pt_{23}$ MSF, which transform, respectively, to equilibrium Zr_5Pt_3 and metastable QC phases. Also displayed are TEM results that further confirm the synchrotron X-ray data.

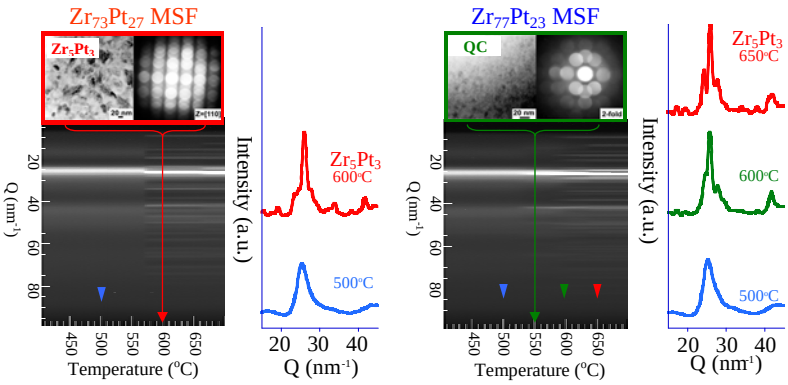

Impact:

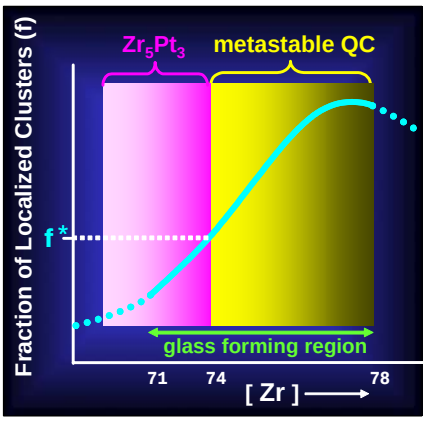

First, the Zr-Pt has proven to be an ideal system to illustrate how subtle changes in composition can dramatically modify a liquid's structure to yield contrasting phase selection during both solidification and devitrification. Second, observing the same transition between equilibrium and metastable phase formation over a small change in Zr content in the MSF strongly emphasizes that the precursor structure leading to a particular phase transformation may be achieved beyond the liquid state. Moreover, it seems unlikely that a 1-2 at% change in a binary composition will be uniform throughout an entire liquid or vapor system, which may suggest that these systems are not homogeneous, but instead contain localized heterogeneities or clusters, perhaps having ISRO, that serve as nucleation centers which increase in number at higher Zr contents. As illustrated above, we consider that a minimum Zr content in Zr-Pt liquids and glasses is required to achieve a critical population of localized clusters (f*), possibly having ISRO, to form a metastable QC phase.

Future Work:

High-energy X-ray scattering studies will be extended to incorporate analysis of pair distribution functions analysis to further understand subtle structural differences currently observed in $Zr_{80-x}Pt_x$ MSR and MSF. These experimental efforts will be augmented by M. I. Mendelev to develop accurate inter-atomic potentials for the Zr-Pt system so that large-scale MD simulations can be used to more closely examine the subtle, yet potent role of composition on equilibrium and metastable phase transformations.

Interactions:

M.J. Kramer (MEPP) and A.I. Goldman (CMP) together with the MUCAT sector of the Advanced Photon Source at Argonne National Laboratory for performing dynamic structural investigations with high energy X-ray scattering in real time and isothermal modes.

[1] Holland-Moritz, D., Mat. Sci. Eng. 2001; A304; 108.
[2] Saida, J. et al,. Appl. Phys. Lett. 2001; 79; 412.
[3] Kelton, K et al., Phys. Rev. Lett. 2003; 90; 19550

Creep Deformation Behavior of Metallic Glasses: Molecular Dynamic Simulations and Experiments

Personnel: S.B. Biner (PI)

Scope:

In this study the creep deformation behavior of metallic glasses was simulated using a two-dimensional binary amorphous model system, and the results were compared with experimental creep deformation results from a Zr-based bulk metallic glass. In spite of the simple model system, the simulations exhibited rich phenomenology analogous to the experiments. Results indicate that the model system exhibits Newtonian flow at low stress levels and power-law creep at high stress levels, as was seen in experiments. The creep deformation proceeded with creation and annihilation events of free volume. The well-known constitutive free volume model unifies the variation of the steady-state strain rates with stress at both regimes of creep deformation, which is in agreement with the suggested theories of the deformation behavior of amorphous systems.

Research Highlights:

The deformation behavior of metallic glasses is usually classified as inhomogeneous or homogenous deformation. The former occurs at temperatures well below the glass transition temperature, where the formation of localized shear bands and very limited ductility are the typical characteristics of this deformation behavior. In contrast, homogenous deformation takes place near the glass transition temperature and exhibits a nearly super-plastic behavior without the localization of deformation. Individual atomic jumps are the basic step in the mechanism of homogenous deformation. In order for individual atomic jumping events to take place, there should be enough free volume in the immediate neighborhood to accommodate the volume of the jumping atom. In the presence of applied stress, such favorable jumps eventually lead to diffusional flow. Furthermore, the applied stresses may cause additional creation of free volume by squeezing the atoms into a smaller available free volume by displacing the surrounding neighboring atoms. However, the newly created free volume is quickly distributed among the neighboring atoms by local rearrangement. This annihilation process is essentially a structural perturbation; therefore, equilibrium between the stress-assisted creation and the kinetically-controlled annihilation of free volume is required for the continuation of homogenous deformation. Stress relaxation and creep experiments with metallic glasses have been used previously to examine homogenous deformation behavior[1]. However, questions still remain concerning the details of the stress-strain rate relationships. In particular, while the experiments conducted at low stress levels exhibit a Newtonian viscous flow, at high stress levels the strain rates correlate with stress in the form of power law creep with a larger stress exponent.

In this work, the simulated amorphous system was a two-dimensional model binary alloy. The interactions between the components are described by 6-12 Lennard-Jones potentials. This model binary system can be quenched into a stable glassy state and also has a quasicrystalline ground state[2]. The experimental creep deformation behavior of a Zr-based metallic glass was studied under constant stress and a temperature 25°C below its glass transition temperature. Figure 1 shows the atomic arrangements after deformation during the molecular dynamics (MD) simulations. Each atom is colored differently based on their strain values and formation of the free volume (open spaces) can be clearly seen by the red arrows. The evolution of homogeneous deformation in the form of dilute shear bands can also depicted from the figure. Figures 2 and 3, respectively, summarize MD and experimental results from steady-state strain rate values obtained at different stress levels. Both simulations and experiments show two regimes of creep deformation: Newtonian flow at low stress

levels and power law creep at high stress levels, where the creep deformation is expressed in the form of Norton's power law (dashed lines).

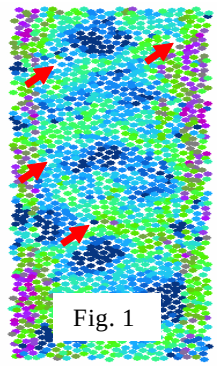

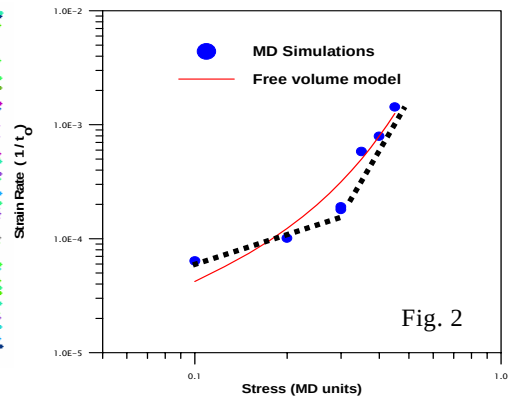

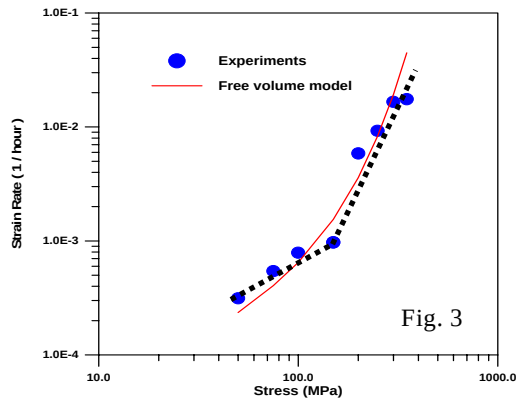

The transition-state theory for amorphous solids[3], based on the free volume, predicts a strain rate-stress relation in the form of:

$$\dot{\varepsilon} = \dot{\varepsilon}_0 \sinh \frac{\sigma \gamma_f \Omega_f}{k_B T}$$

where γ_f is the local strain produced by the shear site of volume Ω_f, k_B is the Boltzmann's constant and T is the temperature[3]. By taking the relative parameters, the predicted steady strain rates from the theory are shown with the solid red lines in Figs. 2 and 3. Both regimes of creep deformation can be described successfully in a unified manner from both the MD simulations and experimental data.

Impact:

These results demonstrate that the evolution of the free volume is the mechanism responsible for homogeneous deformation behavior of amorphous materials such as metallic glasses and, moreover, is the primary reason of the presence of two regimes of creep deformation.

Future Work:

Three-dimensional MD simulations using more realistic EAM potentials under superimposed hydrostatic stress states will be performed to further elucidate the kinetics of free volume evolution and its correlation with the initial structure of the glassy states.

Interactions:

The kinetics of free volume evolution determined from MD simulations is being correlated with X-ray scattering experiments performed by D.J. Sordelet and M.J Kramer at the Advanced Photon Source.

[1] B.S.S. Daniel et al., MRS Symp. Proc. **644,** (2001) L.10.7.1.
[2] F. Falcon et al., Europhys. Lett. **2**, (1986) 625.
[3] F. Spaepen, Acta Metall. **25**, (1977) 407.

Anisotropic Nature of Free Volume Creation in Metallic Glasses During Homogenous Flow

Personnel: D.J. Sordelet (PI), M.J. Kramer (PI), and R.T. Ott (Post Doc)

Scope:

When subjected to isothermal creep deformation, metallic glasses experience strain-induced structural disordering that results in an increase in the excess free volume. Unlike previous research that has focused on the *average* changes in the free volume during deformation, this new effort examines the dependence of the structural changes on the stress state. Using high-energy X-ray scattering, we have found that the free volume creation during homogeneous deformation is *anisotropic*, with the largest amount of excess free volume being distributed along the tensile loading axis. The X-ray scattering results combined with thermal analysis data allow us to more clearly understand the nature of free volume creation during homogeneous flow.

Recent Results:

Inhomogeneous flow in metallic glasses occurs by a deformation-induced disordering of the atomic structure, which is characterized by a shear-induced dilation in the localized regions of deformation[1]. For higher temperatures and lower applied stresses, the deformation occurs in a homogeneous manner. Several studies on metallic glasses deformed at high stress in the homogenous flow regime have also confirmed the presence strain-induced structural disordering through the observation of a drop in the flow stress of the alloys for constant strain rate experiments[2] and accelerating strain rates for constant stress creep experiments[3]. However, these studies have examined only the *average* structural changes associated with homogenous deformation.

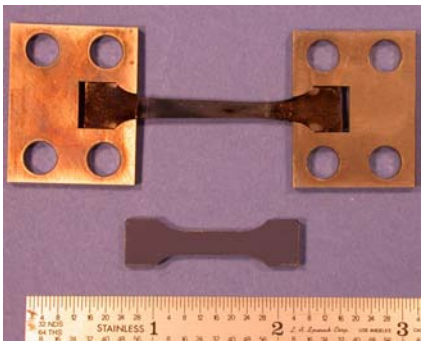

A major objective of this project is to explore the nature of free volume creation in metallic glasses during homogenous deformation. In particular, we are interested in the dependence of the structural changes on the stress state and the amount of strain imparted during deformation. Recently, Yavari and coworkers have used X-ray scattering to measure the average excess free volume in inhomogeneously deformed metallic glasses[4]. To obtain homogeneously deformed samples, we performed isothermal creep experiments in tension. A major advantage of performing the tests in tension is that a broad range of strain levels are generated in the sample, as illustrated by the variance in the cross sectional area of the deformed sample shown in the figure to the right. The gradient of strains along the gauge length provides a convenient means for examining the dependence of the free volume creation on the macroscopic plastic strain. Additionally, the simple uniaxial loading allows us to explore the stress state dependence of the free volume creation and compare the data with MD simulations being performed in parallel by S. B. Biner.

High-energy X-ray scattering experiments were performed at the Advanced Photon Source to measure the excess free volume in the creep samples. The figures on the following page clearly show that the free volume distribution is dependent on the direction of the applied stress. For the longitudinal direction (parallel to loading axis) the free volume increases with increasing macroscopic strain (left image), while the free volume in the transverse direction remains more or less constant. The results suggest that the free volume distribution is anisotropically distributed along the tensile loading axis. The figure on the right

further illustrates the changes in the free volume along the gauge length of the creep sample, as detected by differential scanning calorimetry (DSC). The decreasing heat signal of the glass transition peak indicates a more disordered structure (i.e., highly deformed region ① compared to the unstrained region within the grip area ④), which is consistent with an increase in free volume. Both the X-ray and DSC results show that the structure becomes more disordered as the strain increases in the sample, but the former results clearly illustrate the anisotropic distribution of the free volume.

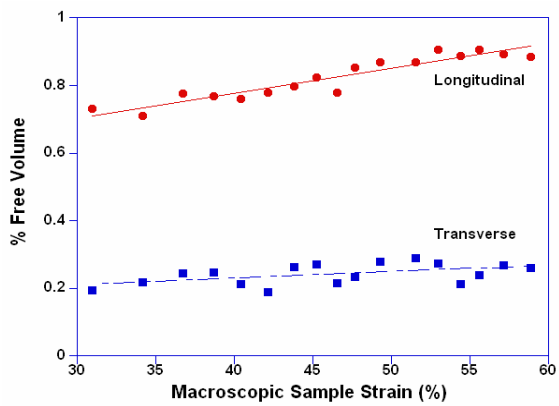

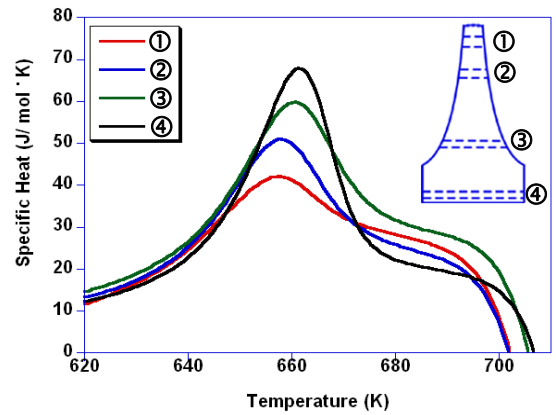

Impact:

The free volume model is commonly used to describe the plastic flow behavior of metallic glasses as well as other properties, which are all controlled by atomic mobility. Therefore, understanding the dynamics of free volume creation during deformation is essential for understanding the mechanical behavior of metallic glasses. This work is helping to link the atomistic structure of metallic glasses with their macroscopic mechanical properties and serves to test and validate ongoing MD simulations of deformation in amorphous systems.

Future Work:

Our X-ray diffraction technique will be further used to examine free volume creation in metallic glasses subjected to more complicated stress states. Of particular interest is examining samples that have been inhomogeneously deformed in loading conditions such as pure shear. If successful, this approach will help us to study the dependence of the free volume creation on the orientation of an applied shear stress. Deforming samples in pure shear may also allow us to use small-angle X-ray scattering to examine if the coalescence of the free volume can be observed, and if so, whether it too shows anisotropic behavior. The ultimate goal is to develop a comprehensive understanding of free volume creation and coalescence in metallic glass alloys by combining these experimental efforts with MD simulations and finite-element modeling, as appropriate.

Interactions:

S. B. Biner at Ames Laboratory is directing and performing the MD simulation and finite element efforts that couple with these experimental techniques. M. Li from Georgia Tech is cooperating by using his large-scale MD simulations to examine atomic motion and bonding changes when homogeneous, uniaxial deformation transfers to a triaxial-type stress state (e.g., during necking in a creep test).

[1] J. Li et al., Phil. Mag. A **82**, 2623 (2002).
[2] P. de Hey et al., Acta Mat. **46**, 5873 (1998).
[3] M. Heggen et al., Mat. Sci. Eng. A **375-377**, 366 (2004).
[4] A. R. Yavari et al., Acta Mat. **53**, 1611 (2005).

Characterization of Yield Conditions and the Embryonic Stages of Shear Band Formation in Amorphous Solids

Personnel: S.B. Biner (PI)

Scope:

The early stages of shear band evolution in a two-dimensional model amorphous system are studied by incorporating an instability criterion into quasi-continuum finite element analyses. The results obtained from these analyses are compared to molecular dynamics simulations and show that the instability criterion successfully predicts the transition from elastic to inhomogeneous plastic deformation by the nucleation of shear bands.

Research Highlights:

The current consensus for the inhomogeneous deformation of amorphous systems is the cooperative behavior of small clusters of randomly close packed atoms, so-called shear transformation zones (STZs). These STZs create a localization of displacements in surrounding regions that triggers the evolution of highly localized shear bands during the deformation. It has been hypothesized that STZs are geometrically identifiable regions in the amorphous solids. Several approaches, ranging from Voronoi constructions to local stress distributions have been adopted to identify the STZs in previous studies. In the current study, we quantified the microstructure to identify the transition from elastic deformation to inhomogeneous plastic deformation in amorphous solids by using a localization criterion. In this criterion, the loss of strong ellipticity in the strain energy function is an indication of the instability in a solid, as first proposed by Hill[1] and later reformulated by Rice[2] by admitting an incremental displacement jump across the discontinuous interface. The localized deformation manifests itself along this interface as slip or shear banding in inelastic materials. Rice's approach can be interpreted mathematically in the simplest form as:

$$\Lambda_{\min} \equiv \min_{|k|=1,|w|=1} \left(C_{ijkl} w_i w_k + \tau_{jl}\right) k_j k_l$$

where, C_{ijkl} is the spatial tangent modulus containing the elastic constants, τ_{jl} is the Cauchy stress and k and w are the two unit vectors. The traction equilibrium across the interface can no longer be sustained when $\Lambda(k,w)$ becomes negative, and the unstable growth of the shear band becomes imminent .

The amorphous system simulated in this study is a two-dimensional model binary alloy described by 6-12 Lennard-Jones potentials. First, the yield surface of this model system is defined by different degrees of multiaxial loadings using molecular dynamics (MD) simulations. We implemented the above instability analysis into a quasi-continuum finite element method (FEM). A FEM mesh was generated from the fully relaxed MD simulations, Fig.1, where the nodal positions of the triangular elements correspond to the atomic positions. The evaluation of the spatial tangent modulus uses the same Lennard-Jones potentials that were used in the MD simulations. Figure 2 shows the variation of the smallest value of $\Lambda_{\min}$ among all the nodes (atomic positions) with the imposed effective strains. As can be seen, $\Lambda_{\min}$ starts with a finite value and decreases towards zero with increasing deformation. A clear transition from elastic to plastic deformation can be discerned on the stress-strain curves obtained from the MD simulations at the strain values where the $\Lambda_{\min}$ reached zero or negative values. Using the instability criterion as the limit of the elastic deformation, the yield values from the quasi-continuum FEM analyses is compared with the resulting yield surface from the purely MD simulations in Fig. 3.

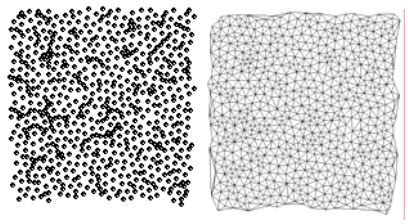

Fig. 1

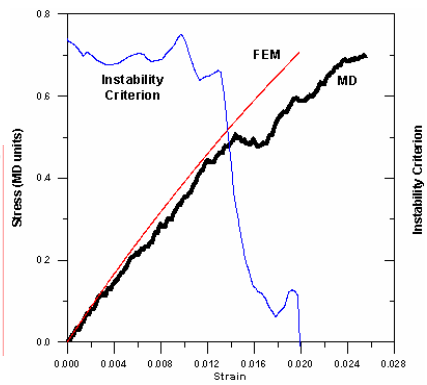

Fig. 2

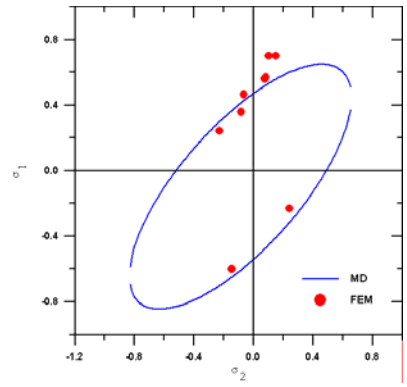

Fig. 3

The spatial variation of the Λ_{min} and effective strain distributions at the instability point obtained both from the MD simulations and the FEM are shown in Figs. 4a and b. For both types of simulations, the close correlation between the distribution of the effective strain and the distribution of the Λ_{min} is visible. The larger values of effective strain occurred at the regions where the Λ_{min} values were smaller and the circle in Fig. 4c indicates either the location of the instabilities (i.e., where the Λ_{min} became zero or negative) or the nucleation sites of the shear bands.

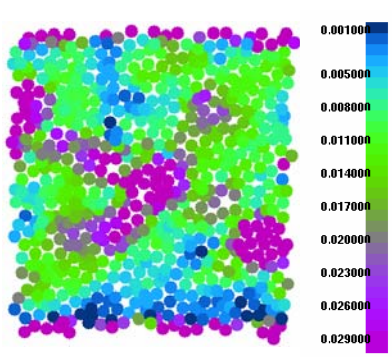

Fig. 4a (MD)

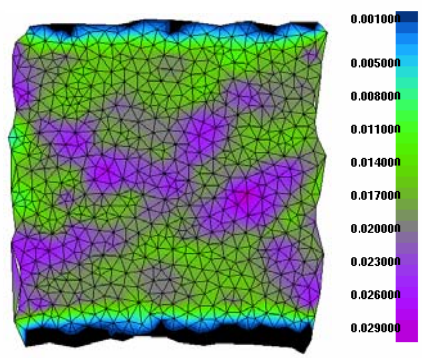

Fig.4b (FEM)

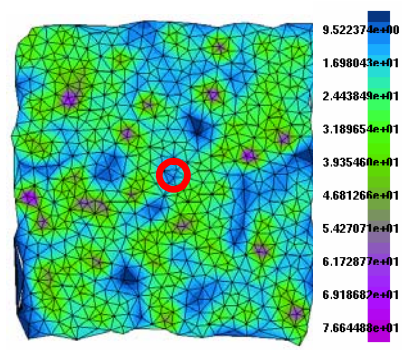

Fig.4c

Impact:

The instability criterion successfully predicts the transition from elastic to inhomogeneous plastic deformation in the form of nucleation of shear bands. The results indicate that the instability criterion can also be used as an effective tool for quantitative characterization of the structures of amorphous systems. Moreover, this work also supports the general opinion that a pressure-dependent yield surface exists for amorphous solids.

Future Work:

The roles of the system size, loading rates and initial amorphous atomic structure obtained with different cooling rates will be further assessed to better understand shear band nucleation and propagation.

[1]R. Hill, "Acceleration waves in solids", J. Mech. Phys. Solids, **10**, 1, (1962).
[2]J.R. Rice, "Localization of plastic flow", Theoretical and Applied Mechanics, Ed. W.T. Koiter, North-Holland Publishing Company, p. 207, (1976).

Synthesis and Characterization of Aperiodic and Related Crystalline Binary Compounds

Personnel: T.A. Lograsso (PI), M.J. Kramer (PI), and D. Wu (Asst. Scientist)

Scope:

This project is focused on the synthesis and characterization of bulk, single grains of binary aperiodic and closely related approximant phases, with a goal of understanding the variations in atomic arrangement and phase stability of these similar structures. The recent discovery of stable, binary quasicrystalline alloys is very exciting since this greatly facilitates the use of various advanced scattering methods to achieve better insight between the structural versus chemical stabilities that has been elusive in ternary and higher-order aperiodic systems.

Research Highlights:

Improvements, modifications and application of synthesis methods to various binary phases (aperiodic and related crystalline) are ongoing. Synthesis of large, bulk single grains of the hexagonal crystalline phase *h*-$Cd_{51}Yb_{14}$ has been accomplished using the Bridgman method. Growth was carried out under controlled solidification conditions in sealed Ta crucibles, which help to maintain compositional integrity by eliminating evaporative losses of Cd and reaction with the containment material. Compositional analysis of the as-grown phase indicates no evidence of macrosegregation along the length of the crystal. Electron microscopy of the hexagonal phase is hampered by the enhanced atmospheric reactivity of the higher Yb content of the hexagonal phase. This high sensitivity to ambient exposure was not observed during recent synthesis and TEM studies of the quasicrystalline $Cd_{5.7}Yb$ or cubic approximant Cd_6Yb phase. High-resolution TEM examination in single grains of the *h*-$Cd_{51}Yb_{14}$ phase revealed a fine distribution of a second phase that exists throughout the hexagonal matrix. High-energy X-ray experiments at the Advanced Photon Source using both powdered and bulk single-crystal samples of the *h*-$Cd_{51}Yb_{14}$ phase confirmed the bulk nature of the second phase, Fig. 1. These precipitates have no orientational relationship to the matrix. Moreover, identification of this fine structure by d-spacing comparisons indicates the precipitates are pure Cd, possibly formed by the selective oxidation of Yb.

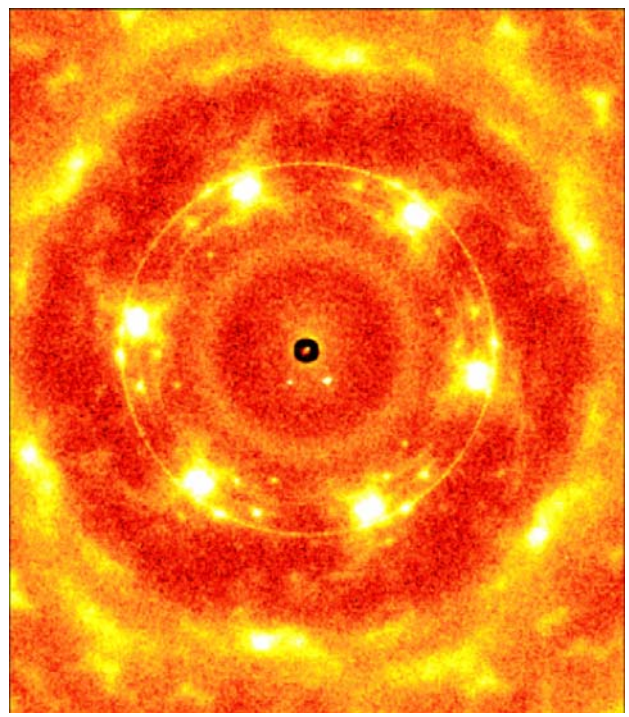

Fig. 1 X-ray transmisson experiments at the APS showing Debye-Scherrer rings from second phase in bulk single crystalline $Cd_{51}Yb_{14}$.

Elastic constants, their temperature and pressure derivatives, and coefficients of thermal expansion of the icosahedral quasicrystal *i*-$Cd_{84}Yb_{16}$ and hexagonal *h*-$Cd_{51}Yb_{14}$ phases were studied by resonant ultrasound spectroscopy, conventional ultrasonic resonance techniques and dilatometry, respectively. The elastic properties of both phases are very similar although they are structurally not related. Contrary to the

assumption often found in quasicrystal literature, the similarity of particular physical properties is not necessarily an indication for structural similarity. Furthermore, a first-order phase transition at about 111 K was observed in *h*-$Cd_{51}Yb_{14}$, as indicated by a reversible discontinuity in the thermal expansion in Fig. 2. This phase transition is related to ordering of the orientationally-disordered Cd tetrahedral in the centers of the clusters.

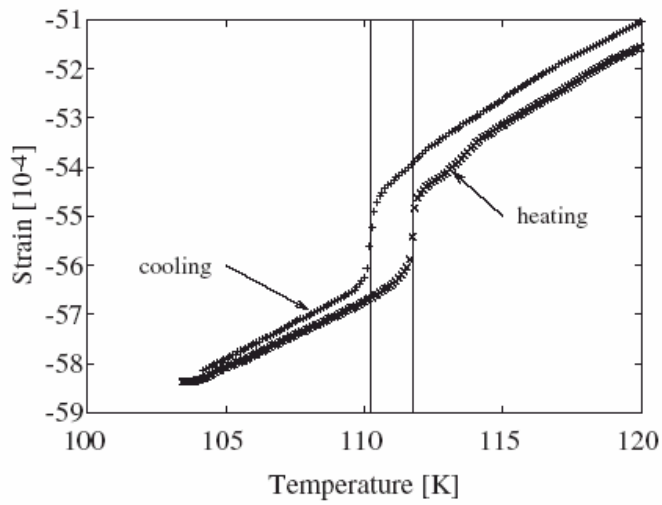

Fig. 2 Thermal expansion of $Cd_{51}Yb_{14}$ illustrating reversible first-order phase transition.

Impact:

The intrinsic properties of icosahedral quasicrystal *i*-$Cd_{84}Yb_{16}$ and hexagonal *h*-$Cd_{51}Yb_{14}$ phases have been accurately determined. Moreover, the advanced processing techniques and synthesis routes stemming from this and other studies in the Ames Lab are now being practiced by many groups throughout the world to make high-quality single grains of quasicrystalline and approximant compounds. The availability of high-quality, well-characterized single crystals of these compounds has facilitated the understanding of the intrinsic structural complexities and properties of these novel materials. Another achievement has been the sharing of high-quality quasicrystal samples for collaborative research in over 30 laboratories throughout the world, thus allowing the field to advance at a pace faster than otherwise possible.

Future work:

Our current goal is to modify synthesis techniques to enable subsequent characterization of large, single grains of the 2/1 approximant phase in Cd-Yb system, along with quasicrystalline and approximant phases in the Cd-Ca system. The synthesis route for large, single grains of 2/1 $Cd_{76}Yb_{13}$ approximant is being developed and refined. Methods used for the Cd-Yb growth will be applied to the Cd-Ca system with appropriate modifications to yield single-phase, single grains of aperiodic and periodic phases to assist in the development of structural models of these phases and to correlate similarities between aperiodic and periodic phases. Detailed TEM and structural analyses will be extended to the Cd-Ca alloy system where differential phase contrast is likely to be realized from the substitution of ytterbium by calcium.

Interactions:

We are collaborating with W. Steurer at ETH Zurich, Switzerland by synthesizing single-grain samples of QC and related approximant systems for their structural characterization and physical property measurements. In addition, L.S. Chumbley of the MSE Dept. at Iowa State University is contributing to this work by performing TEM studies of Cd-Yb approximant phases.

Quasicrystalline $Cd_{84}Yb_{16}$ and its Cd_6Yb Cubic Approximant Phase: A Model System for 3-Dimensional Quasicrystals

Personnel: M.J. Kramer (PI), T.A. Lograsso (PI), Y.Q. Wu (Post Doc) and D. Wu (Asst. Scientist)

Scope:

Stable, binary phases having aperiodic, quasicrystalline structures together with their related crystalline approximant phases provide an intriguing opportunity to gain better insight into structural versus chemical stabilities which has been elusive in ternary and higher-order systems. The complexity of performing site occupation determinations in a binary compound is considerably reduced compared to ternary systems. The general simplicity of a binary system presents numerous advantages in both computational and experimental investigations of structure. Therefore, binary phases are ideal candidates to study for constructing 3D structural models of quasicrystalline compounds. Using high-resolution transmission electron microscopy and image simulation techniques, we are able to compare the local atomic structures of selected quasicrystalline and approximant phases. A unique polyhedral packing is present in both compounds, but the manner in which these nested polyhedrons are arranged into 3D space dictates whether an aperiodic or a periodic atomic structure manifests in the bulk solid.

Research Highlights:

There is a strong correlation in the local order on the atomic scale between a single-grain $Cd_{84}Yb_{16}$ quasicrystal (QC) and its corresponding Cd_6Yb approximant (AP) phase. High-resolution transmission electron microcopy (HRTEM) of the QC and the AP phases coupled with image simulation techniques were used to construct a model for the 3D QC phase based on edge-sharing of four-shell clusters along the 2-fold directions. The resulting model shows how the aperiodic packing can develop in the primitive icosahedral phase. The cubic Cd_6Yb AP phase (*Im*3 structure) has a very large unit cell (a = 15.64 Å) and consists of a body-centered-cubic packing of the clusters. Both the QC and AP phases have atomic shells with icosahedral symmetry around their centers, Fig. 1. Oriented TEM/HRTEM specimens were sectioned from larger single grains synthesized at Ames Laboratory and electrolyte-polished to make final HRTEM specimens. Special care had to be taken to minimize air exposure due to rapid surface oxidation of the Yb-containing materials. Microscopy was performed along two sets of common axes: the [001] of the AP phase and the two-fold of the QC phase. In addition, the [530] direction of the AP phase, which approximately corresponds to a five-fold axis in the QC, were also examined. In order to model such a large unit cell with a high-index zone axis, a 'pseudo-unit cell' having dimensions of 15.64 Å by 21.46 Å with a variable thickness in the beam direction, was constructed and then modeled as a layered structure.

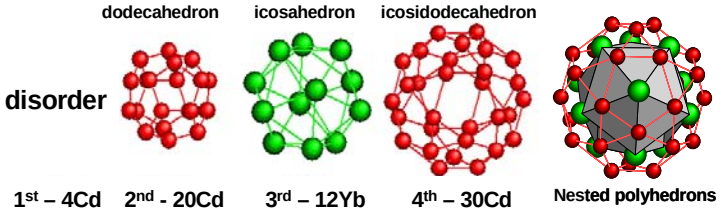

Fig. 1 The nested polyhedra of the Cd-based QC are comprised of an inner shell that appears disordered in the QC phase, but ordered in the AP phase. The polyhedra are chemically ordered with the larger ion (Cd or Yb) forming an icosahedron.

The similarities in the 5-fold orientations between the two phases are readily observed in Fig. 2. Ten-fold pin-wheel-like structures are periodically or aperiodically arranged for the AP and QC phases, respectively. These pin-wheel features are formed by the nested arrangement of the dodecahedron and icosidodecahedron Cd shells and the intervening Yb icosahedron. How these cluster structures link to the

next cluster determines the periodicity, or the lack of it. In the case of the AP phase, these clusters are linked along the <111> direction by 36 additional Cd atoms filling out the unit cell of 144 Cd and 24 Yb atoms. These clusters are shown to pack more closely in the QC phase by shifting to one of three <1+τ,τ,1> directions (i.e., the non-orthogonal 2-fold directions), where τ is the Golden Mean ($\frac{1+\sqrt{5}}{2}$). This accounts for the three different spatial separations of the clusters since there are three unique two-fold directions in projection along the 5-fold axes. Rotational symmetry is preserved during these shifts while translational symmetry is eliminated. As a result, clusters are able to pack slightly closer together in the QC structure than in the AP phase, which is consistent with the QC phase's slightly higher density (8.86 vs 8.41 g/cm^3). This packing arrangement also appears to be consistent in the 2/1 $Cd_{76}Yb_{13}$ approximant.

Impact:

The present studies show that the local order of binary $Cd_{84}Yb_{16}$ QC and its corresponding $Cd_{86}Yb_{14}$ AP phase may be reconstructed based on a model of the bcc Cd_6Yb approximant structure. Using HRTEM techniques a very high degree of similar structural perfection between the 5- and 2-fold directions of the QC phase and the approximant phase's structure along <τ10>, ~ [530], and [100] directions were observed. Image simulation on the bcc approximant agrees very well with the HRTEM observations. Solutions to earlier QC structures were hampered by the complexities of ternary or higher-order compositions. These well-ordered, binary aperiodic phases and their chemically similar periodic approximants are providing unprecedented opportunities for studying and understanding the nature of quasicrystal formation.

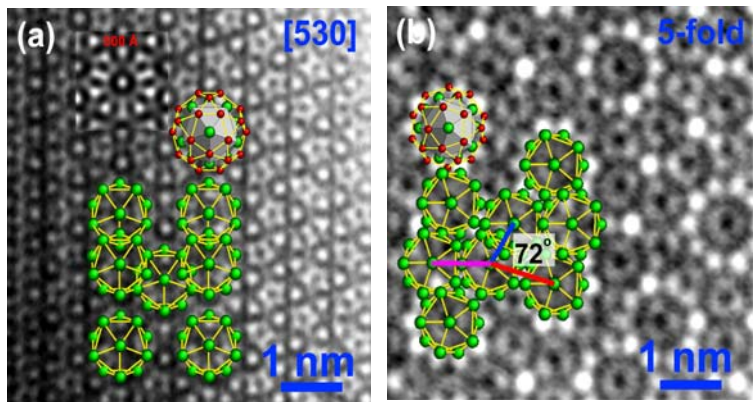

Fig. 2 HRTEM images of the AP (a) and QC (b) along the [530] and 5-fold axes respectively. The result of the multsclice calculation for the AP phase at 80 nm defocus is shown as an inset near the top. The cluster structure is shown as follows: The Yb atoms are green with yellow lines connecting the atoms which form an icosahedron (outline in grey) while the Cd atoms, which form the isododecahedron cluter, are shown in red. To simplify the 2D projection along the 5-fold axis of these nested clusters, only the Yb icosahedron are shown. In the AP phase, the Yb icosahedrons form a bcc lattice, part of which is shown above. The QC phase shows the tighter packing of these icosahedron clusters and the shift along the 2-fold direction giving rise to the 5-fold rotation symmetry.

Future Work:

There are a number of related compounds which are isostructural to the Cd-Yb system, in particular Cd-Ca. The Yb^{2+} and Ca^{2+}, while similar in size, have different scattering cross-sections for X-rays, which will exploited to obtain more precise structure determinations. In the Ca-Yb system, the 2/1 AP (*Pm*3) has a large unit cell (25.329 Å) that appear to be more closely related to the QC phase than the AP structure in the Cd-Yb system. However, it is not yet known if the Ca-Yb is a stable or metastable phase, or if it can be synthesized into large single grains. Synthesis studies will be performed to determine the feasibility of producing and utilizing this very desirable system.

Liquid Structure of the $Cd_{84}Yb_{16}$ Quasicrystalline-Forming Compound: Implications of Icosahedral Order in Liquid Metals

Personnel: M.J. Kramer (PI), T.A. Lograsso (PI), D.J. Sordelet (PI), M.F. Besser (Asst. Scientist) and D. Wu (Asst. Scientist)

Scope:

There has been a revival recently in the half-century old hypothesis by Frank predicting icosahedral short-range order (ISRO) in liquid metals. While a number of recent publications claim ISRO in both elemental liquids and compounds related to quasicrystalline phases, our observation of the lack of any obvious ISRO in a binary $Cd_{84}Yb_{16}$ liquid that congruently forms the primitive icosahedral quasicrystalline phase underscores the complexity of metallic alloy solidification. Moreover, these results question the universality of Frank's hypothesis and suggest that some refinement to the concepts should be considered.

Research Highlights:

The structure of single-grain $Cd_{84}Yb_{16}$ quasicrystalline (QC) samples aligned along the 2- and 5-fold axes was studied from 300 to 1050 K using high-energy synchrotron X-rays, Fig. 1. The QC phase is stable up to its melting temperature of 914 K and has a large linear thermal expansion coefficient of 37.1 ppm/K over this temperature range. The samples melt congruently over a temperature range of less than 1 K. The liquid is 7% less dense than the solid, and upon cooling from the melt, the quasicrystal phase directly solidifies within that 1 K interval under equilibrium conditions. However, under natural cooling conditions ~ 5 to 25 K of undercooling can be achieved, depending on the cooling rate. In addition to temperature-dependent structure factor determinations using synchrotron radiation, neutron diffraction studies were performed in this study using both natural abundance Cd and isotopically enriched Cd^{112} to obtain partial pair correlations.

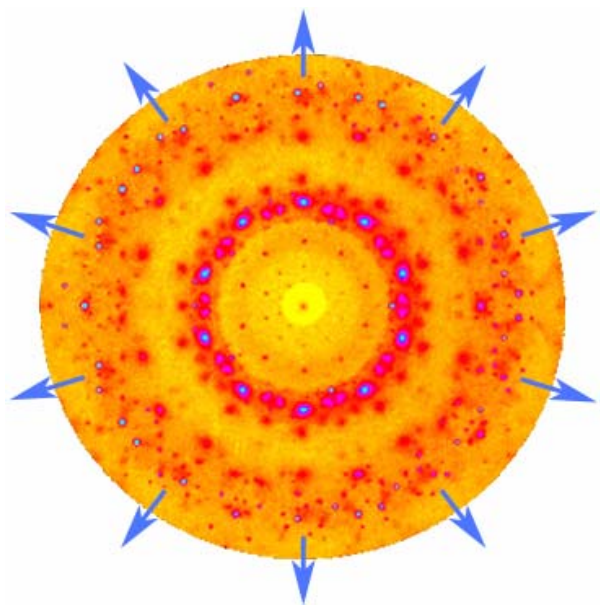

Fig. 1 2D X-ray diffraction image from the 5-fold axis of a $Cd_{86}Yb_{14}$ QC sample heated up to ~1 K below its melting temperature.

The liquid's density change was linear over the 175 K of superheat that was explored, Fig. 2. The calculated temperature dependence on the packing density of the melt is smaller than that for either elemental Cd or Yb. A linear thermal expansion of the liquid density was calculated to be -94.2 ppm/K, slightly less than the calculated isotropic density change of -112.9 ppm/K for the quasicrystalline solid. Interestingly, there is a large decrease in the density upon melting. One reason for this large decrease may be the possibility of close Cd-Cd bonds in the $Cd_{84}Yb_{16}$ primitive icosahedral structure. The innermost shell of the cubic approximant is believed to be disordered while the 2nd and the 4th shells are comprised only of Cd atoms. The Yb atoms reside only in the 3rd shell, which is an icosahedron. In terms of the pair-pair correlations, there are few Yb-Yb nearest neighbors. The 2nd and 4th shells are connected through Cd-Yb bonds. If the stability of the Cd-Yb phases is enhanced by the hybridization of the Yb d-states with the wide Cd sp-band, then the liquid structure should be dominated by a similar distribution of

Cd-Cd and Cd-Yb bonds as in the solid. The pair distribution function of the Cd-Yb liquid obtained from a reverse Monte Carlo simulation, Fig. 3, shows asymmetry in the first pair-pair distribution, which is consistent with the shorter Cd-Cd and slightly longer Cd-Yb bonds that are ~ 3.0 Å and ~ 3.4 Å, respectively. In fact, the atomic pair distribution function for the liquid shows a striking similarity to that of the cubic 1/1 approximant, where we have established that the local structure of the QC is identical to that of the Cd_6Yb approximant. By association, the partial pair correlation distances of the Cd_6Yb approximant should be a very close analogue to the liquid of the $Cd_{84}Yb_{16}$ QC phase. The weaker temperature dependence of the packing density of the Cd-Yb liquid compared to either Cd or Yb suggests strong Cd-Yb bonding even in the liquid. Since Cd_6Yb, which is the crystalline analogue, already shows a broad distribution of Cd-Yb second nearest neighbors, the broad distribution observed in the liquid should be due to loss of the strong Yb-Yb correlations. This is very intriguing since it is the retention of strong second nearest-neighbor correlations that is believed to give rise to icosahedral ordering in metallic liquids. If the ISRO is dependant on how centralized point-like atomic packing becomes, then as the inter-atomic potentials become more angularly dependent, the liquid should exhibit less ISRO. If this is true, then liquid Cd and Yb should each have relatively strong ISRO. However, ISRO is not readily observed in the published structure factors for the liquid state of either of these two elements.

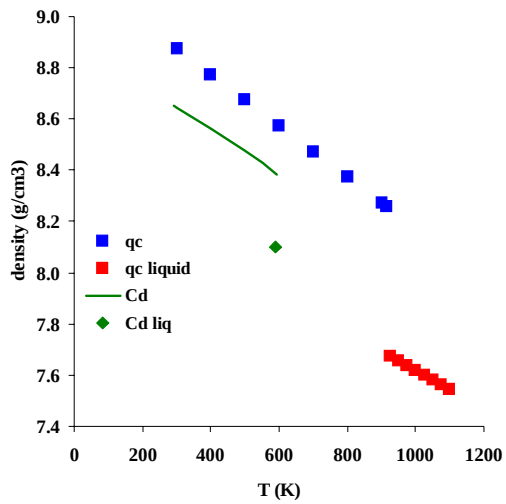

Fig. 2 Measured density change in the $Cd_{84}Yb_{16}$ QC phase through its melting point at 914 K. The change in the density of Cd is shown for comparison.

Impact:

Understanding what influences the SRO of metallic systems is crucial for being able to develop rational models for solidification. Unlike recent results indicating that simple metallic liquids, which have ISRO, solidify into crystalline compounds (i.e., consistent with Frank's hypothesis) this congruently melting quasicrystal appears to form a liquid without ISRO. This provides an explanation for the observed slow nucleation rate of this stable quasicrystal. Quantifying the differences in liquid and solid structures and interfacial free energies is critical for developing rigorous solidification models.

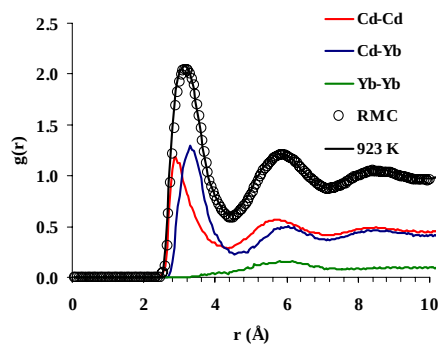

Fig. 3 Partial pair correlations based on reverse Monte Carlo fitting of experimental data.

Future Work:

Binary systems are better suited to molecular dynamic simulations than the more common quasicrystalline forming phases having three or more elements. Using the Vienna Ab Initio Package, simulations of the liquid state are currently underway. Preliminary results show good agreement with the reverse Monte Carlo results.

Interactions:

Neutron diffraction experiments are being performed with U. Dahlborg of the CNRS in Nancy, France and G.J. Cuello of Institut Max von Laue - Paul Langevin (ILL) in Genoble, France. Ab initio simulations are being performed by J.R. Morris at ORNL.